Interface Stability and the Growth of Optical Quality Perovskites on MgO

R. A. McKee, F. J. Walker,* E. D. Specht, G. E. Jellison, Jr., and L. A. Boatner
Oak Ridge National Laboratory, Oak Ridge, Tennessee 37831-6118

J. H. Harding
Theoretical Studies Department, AEA Industrial Technology, Harwell Laboratory, Didcot, Oxon OX11 ORA, United Kingdom
(Received 16 July 1993)

An understanding of heteroepitaxy between perovskite and alkaline earth oxides is developed in terms of ion size and interfacial electrostatics. Interfacial energy minimization at the first atomic layers is the basis for a commensurate, unit-cell stability. This unit-cell stability presents the opportunity to study reduced dimensional or two-dimensional phenomena in thin-film ferroelectrics and is the basis for growth of high crystal quality, μm-thick films for optical device applications.

PACS numbers: 68.35.Bs, 68.55.Bd, 77.55.+f, 78.66.Li

There have been numerous studies in recent years of the growth kinetics and microstructures of thin-film oxides. While the superconducting perovskite oxides are certainly the most widely studied [1–5], substantial efforts have also been devoted to the study of technologically important ferroelectric perovskites like $BaTiO_3$ and $PbTiO_3$ [6–10]. In all of this work, however, very little clarity has evolved in the understanding of relationships between interfacial structure and crystal quality. This issue is an important one since many of the applications for which the materials might be chosen depend on long range structural coherence. If the appropriate crystal quality could be obtained for thin-film $BaTiO_3$ supported on MgO, for example, or for an integrated $BaTiO_3$/MgO structure on silicon or GaAs, then the optimum optical guided wave (OGW) device structure might be realized [11]. In this Letter we will show that heteroepitaxy for simple oxides can be understood by considering a layer-by-layer energy minimization associated with interfacial electrostatics. We will use the examples of $SrTiO_3$ and $BaTiO_3$ to illustrate that a commensurate, stable interface structure exists with MgO. The stability of this interface structure makes it possible to study two-dimensional phenomena for perovskite oxides that are only a single unit cell high or to grow thick adherent films with good optical quality for device applications. The crystal and optical quality that we will describe does not result from incremental improvements in previously published methods, but rather is attained by directly addressing the fundamental requirements of interfacial energy minimization between perovskite and alkaline earth oxides. We believe that these results have broad implications in developing a comprehensive explanation of oxide heteroepitaxy.

To appreciate how the interfacial electrostatics issue arises in oxide heteroepitaxy, consider the structure of the perovskite oxides. The distinguishing structural characteristic of the perovskite oxide class is recognized as a closest packing of large cations and oxygen anions arranged as stacked sheets normal to a [111] direction. The octahedral interstices that form as a result of this sheet-stacking sequence are in turn filled with higher valence, smaller cations. The resulting structures are cubic with low-index stable crystal faces. The naturally occurring crystal truncations are {001} and are then, for example with $BaTiO_3$, either BaO planes or TiO_2 planes. The ion sizes and charges in these planes are distinctly different, and the initiation of a heteroepitaxial growth sequence for such a structure on another insulating oxide must take this into account. For our example of $BaTiO_3$ on (001) MgO, heteroepitaxy can be accomplished with a unique layering sequence that begins at the TiO_2 plane of the perovskite structure. This layering sequence is a requirement for single-orientation, epitaxial growth of a perovskite on MgO.

While it is not possible in the present context to describe in detail the characterization of the interface structure, the basic features are summarized as follows: For a heteroepitaxial transition between insulating oxides, the interface electrostatics (ion-ion near-neighbor interactions) of the first layers critically determine whether a commensurate structure can develop. For example, in going from MgO to $BaTiO_3$ on the (001) face of MgO, if the transition is initiated at a barium oxide plane, the structure at the interface cannot develop commensurately with the MgO surface. The basic incompatibility results from the large ion-size difference between barium and magnesium. The Mg^{2+} ion is only 0.130 nm in diameter and is accommodated easily in the interstices of oxygen octahedra in the NaCl-type MgO structure [12]; Fig. 1(a) shows this geometrically. The O-O distances along the vertices of the oxygen octahedra containing the Mg^{2+} are 0.297 nm; this distance is very nearly a closest packing separation distance for the O^{2-} ion with its 0.140 nm radius. In the BaO plane of the perovskite, $BaTiO_3$, the equivalent O-O distance is expanded approximately 35% to 0.398 nm as a direct consequence of the 0.274 nm diameter Ba^{2+} ion. The large lattice energy increase that would result from a barium-ion substitution for magnesium in the normal stacking sequence of (001) MgO simply cannot be accommodated and is, of course, not observed as a solid solution or as a commensurate, heteroep-

0031-9007/94/72(17)/2741(4)$06.00

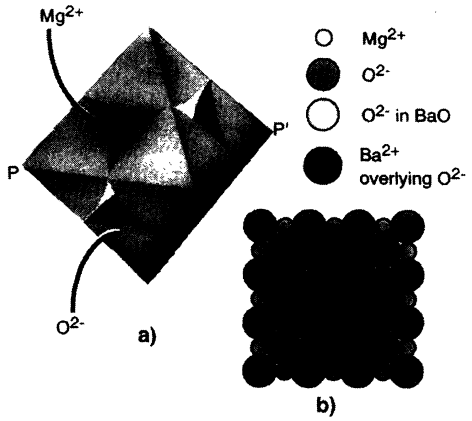

FIG. 1. Size effects, stacking sequence. (a) oxygen oxtahedra showing Mg^{2+} coordination; *P-P'* is [100]; (b) (001)MgO with 45°-rotated BaO layer at anion-anion overlap position.

itaxial system [13,14]. One might argue, however, that the near equivalence of the 0.595 face diagonal distance on (001) MgO and the 0.554 nm cube edge of BaO would facilitate heteroepitaxial growth; such a structure is illustrated in Fig. 1(b). It would not be unreasonable for the resulting 6% lattice mismatch to be accommodated by strain or to be relieved by periodic edge dislocations. However, this simple lattice-matching model contains a critical flaw; a 45°-rotated stacking sequence initiated at a BaO plane leaves either all the barium ions on top of magnesium sites or all the oxygen ions on top of oxygen sites. For example, in Fig. 1(b) we show a configuration that positions the Ba^{2+} cations above O^{2} anions. While these are the low-energy sites for barium, this configuration leaves all of the O^{2} anions in the BaO layer directly on top of O^{2} anions in the underlying MgO surface. Clearly such near-neighbor ion configurations where either cation-cation or anion-anion repulsive interactions occur in such large numbers lead to a high interfacial energy and an inherent instability. A related instability problem in surface physics has been treated by Colbourn, Mackrodt, and Tasker [15] and by Tasker, Colbourn, and Mackrodt [16] in connection with basic theory approaches to interfacial equilibrium and surface segregation phenomena for the alkaline earth oxides. While heteroepitaxy between alkaline earth and perovskite oxides was not considered, the clear result emerged in these theoretical studies that no single-layer coverage of BaO on MgO existed that was energetically stable. We find experimentally that this is of paramount importance to the growth of single-orientation perovskites on MgO.

With the molecular beam epitaxy (MBE) process we deposited barium metal and oxygen at a substrate temperature of 500 °C to form BaO at a $\frac{1}{2}$ monolayer coverage based on the MgO surface; *this is equivalent to 1 monolayer of BaO in* $BaTiO_3$. The high interfacial energies that would result from commensurate BaO epitaxy on MgO should drive some mechanism for lowering the interfacial energy. Figure 2 shows a cube model of the interface and associated reflection high-energy electron diffraction (RHEED) patterns from clean and $\frac{1}{2}$ monolayer BaO-covered (001)MgO surfaces. The implication of the surface segregation theories [15,16] is that "island-like" nucleation of incommensurate BaO-type structures should develop, and this does occur. The cube model in Fig. 2(a) shows an idealization of parallel and 45°-rotated morphologies of an (001) interface between MgO and BaO, and Figs. 2(b) and 2(c) show diffraction patterns as experimental confirmation of their existence. The RHEED pattern in Fig. 2(b) results from an MgO surface prepared in the MBE system by growing 100 nm of MgO homoepitaxially on (001)MgO. The 0,0 and allowed 0,2 surface rods are seen. In Fig. 2(c) surface diffraction at the same zone axis as illustrated but is modified by a single-layer-coverage BaO deposition. As can be seen, incommensurate crystallite orientations have formed and give rise to diffraction at what would be the 0,2 rod position for cube-on-cube BaO and at the 1,1 rod of 45°-rotated BaO as well. Moreover, in addition to the rod spacing indicating the microstructural characteristics of the interface, the diffraction intensity is modulated along the reciprocal lattice BaO rods in a Bragg-like manner; i.e., three-dimensional diffraction occurs that is

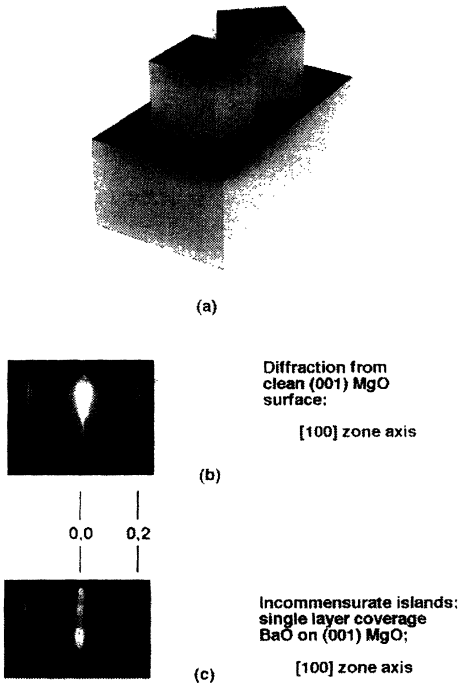

FIG. 2. Incommensurate nucleation and growth of BaO on (001)MgO. (a) Cube model of two orientations; (b) RHEED from the [100] zone axis of clean MgO; (c) RHEED from $\frac{1}{2}$ monolayer BaO-covered MgO.

indicative of "islanding" or surface roughening. These multiorientation, three-dimensional island structures defeat any attempt at growing optical-quality, thick perovskite films.

Figure 3 provides an illustration of the dramatically different result that can be obtained by moving up one plane in the $BaTiO_3$ unit cell to the TiO_2 plane and initiating the growth sequence at that point. A commensurate, atomically flat layer of TiO_2 can form in which every other cation row is vacant over the underlying Mg^{2+} sites. This TiO_2 truncation of (001) MgO satisfies the electrostatic requirements for anion-cation near-neighbor pairs at the interface and is a low-energy, stable truncation of the MgO surface. The missing row of cations in this layer provides the energetically favorable sites for subsequent barium-ion attachment to the crystal surface. As the perovskite growth is continued with alternating barium- and titanium-deposition cycles, $BaTiO_3$ grows layer by layer, and strain relief can occur by nucleation of simple edge dislocations maintaining the single-orientation cube-on-cube epitaxy [17,18]. The $BaTiO_3$ lattice parameter relaxes to its strain-free, bulk value within 10 unit cells from the original interface. The transition from heteroepitaxy to homoepitaxy of the perovskite is completed with the desired single-orientation material and its advantageous long range structural coherence. With the transition from heteroepitaxy to homoepitaxy accomplished in the manner described above, we find that growth rates of the order of 1 μm/h can be attained at temperatures as low as 500 °C by codeposition of barium and titanium or strontium and titanium with oxygen arrival rates equivalent to pressures of 10^{-7} torr.

Figure 4 shows RHEED data accumulated at the [100] zone axis of the starting MgO surface and similarly at the [100] zone axis of relatively thick $BaTiO_3$ films. The $BaTiO_3$ RHEED pattern in the middle panel is from a 100 nm film grown using layer-by-layer energy minimization starting at the TiO_2 layer. The $BaTiO_3$ RHEED pattern in the lower panel is from a 100 nm film grown starting with an incommensurate BaO/MgO interface. In both films the cube-on-cube epitaxy predominates, but multiorientation material is clearly evident with a highly disordered surface and even polycrystalline material contributing to the diffraction pattern in the lower panel. The 100 nm thick $BaTiO_3$ film that gives rise to the RHEED pattern in the lower panel progressively worsens as film growth continues. The surface quality and single-mode growth characteristics of the film imaged in the middle panel allow $BaTiO_3$ to be grown to thicknesses required for optical applications. The surface diffraction in the middle panel arises from a single Laue zone with a surface mosaic or coherence length comparable to the initial MgO surface shown in the upper panel. These homoepitaxy results, although obtained after a heteroepitaxial transition for film growth on an MgO surface, are

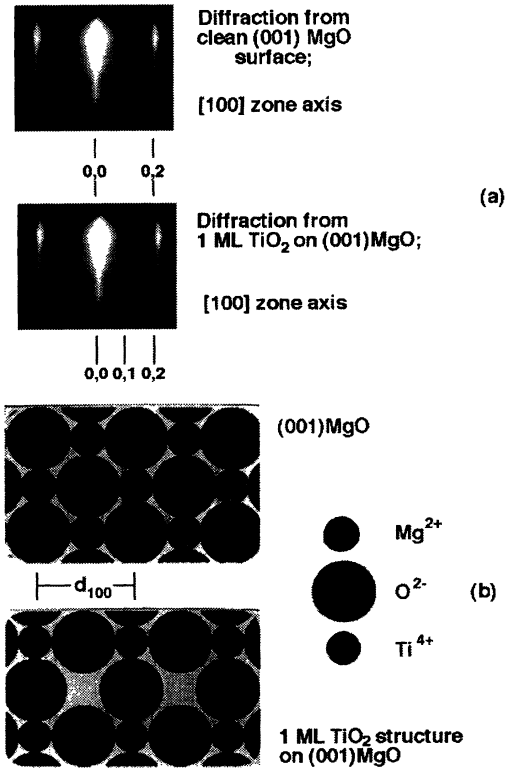

FIG. 3. TiO_2 truncation of (001) MgO. (a) RHEED at the [100] zone axis for clean and TiO_2-truncated MgO; (b) ball models of (001) surfaces.

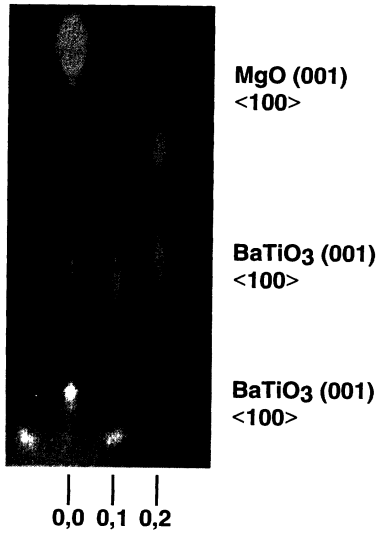

FIG. 4. RHEED data for MgO and $BaTiO_3$. Upper panel: clean MgO (100 nm homoepitaxial growth on polished surface); middle panel: 100 nm $BaTiO_3$ grown on TiO_2-truncated MgO; lower panel: 100 nm $BaTiO_3$ grown on BaO-truncated MgO.

TABLE I. In-plane and out-of-plane x-ray data and index of refraction data for $SrTiO_3$ and $BaTiO_3$ thin films on MgO.

	$SrTiO_3$/MgO	$BaTiO_3$/MgO
Thickness, nm	515	610
Lattice parameter		
In-plane	0.3898 nm	0.4000 nm
Out-of-plane	0.3913 nm	0.4020 nm
Rocking curve width		
In-plane	0.37° FWHM	0.40° FWHM
Out-of-plane	0.62° FWHM	0.70°FWHM
Index of refraction		
@ 632 nm	2.379	2.437

of a similar quality and are entirely consistent with those reported by Terashima *et al.* [19] for a codeposition study of $SrTiO_3$ on (001)$SrTiO_3$. Structural and optical characteristics of the resulting thin films are given in Table I. Walker *et al.* [20] are reporting waveguide-loss data for these materials, and will demonstrate that optical loss coefficients, both in absolute magnitude and wavelength dependence, rival those of $LiNbO_3$. These epitaxial, thin-film structures are of high optical clarity and can be directly compared with $LiNbO_3$, the most commonly applied material in EO devices.

We have shown that ion size and electrostatics at the first atomic layers of the interface between simple perovskites and MgO are the predominate influences on heteroepitaxial growth of these oxides. This is the first time that heteroepitaxy for this important class of oxides has been explained at this level. Both $BaTiO_3$ and $SrTiO_3$ can be stabilized as single orientation, commensurate thin films on MgO at unit-cell thicknesses. The stability of such unit-cell structures presents the opportunity to study reduced dimensional or two-dimensional phenomena in thin-film ferroelectric perovskites. Moreover, by using the TiO_2-truncated MgO surface, optical quality, thin-film ferroelectrics can now be grown to the μm thicknesses required for their application in EO devices. The layer-by-layer MBE process that we have described here for stabilization of the interface between a perovskite oxide and the alkaline earth oxide MgO provides a unique opportunity to exploit the electro-optic properties of thin-film epitaxial ferroelectrics in wave guide applications.

The authors wish to express their appreciation to Kathi Alexander and Gene Ice for their careful reading of the manuscript. Research was sponsored jointly by the U.S. Air Force Office of Scientific Research under interagency agreement DOE No. 1854-A077-A1, USAF No. AFOSR-ISSA-92-0003, by the U.S. Air Force under interagency agreement DOE No. 1692-C123-A1, USAF No. WRDC FY1457-92-N5024, and by the Division of Materials Sciences, U.S. Department of Energy under Contract No. DE-AC05-84OR21400 with Martin Marietta Energy Systems, Inc.

*Also at the University of Tennessee, Knoxville, TN 37996.

[1] J. Kwo, M. Hong, D. J. Trevor, R. M. Fleming, A. E. White, R. C. Farrow, A. R. Kortan, and K. T. Short, Appl. Phys. Lett. **53**, 2683 (1988).
[2] Q. Li, O. Meyer, X. Xi, J. Geerk, and G. Linker, Appl. Phys. Lett. **55**, 310 (1989).
[3] B. H. Moeckly, S. E. Russek, D. K. Lathrop, R. A. Buhrman, Jian Li, and J. W. Mayer, Appl. Phys. Lett. **57**, 1687 (1990).
[4] M. Kanai, T. Kawai, and S. Kawai, Appl. Phys. Lett. **57**, 198 (1990).
[5] D. K. Fork, D. B. Fenner, R. W. Barton, J. M. Phillips, G. A. N. Connel, J. B. Boyce, and T. H. Geballe, Appl. Phys. Lett. **57**, 1161 (1990).
[6] K. Iijima, S. Kawashima, and I. Ueda, Jpn. J. Appl. Phys. **24**, 482 (1985).
[7] F. Fujimoto, Y. Kobayashi, and K. Kubota, Thin Solid Films **169**, 249 (1989).
[8] Z. Surowiak, Y. S. Nikitin, S. V. Biryukov, I. I. Golovko, V. M. Mukhortov, and V.PO. Dudkevich, Thin Solid Films **208**, 76 (1992).
[9] Z. C. Feng, B. A. Kwak, A. Erbil, and L. A. Boatner, Appl. Phys. Lett. **62**, 349 (1993).
[10] H. A. Lu, L. A. Wills, G. W. Wessels, W. P. Lin, T. G. Zhang, G. K. Wong, D. A. Neumayer, and T. J. Marks, Appl. Phys. Lett. **62**, 1314 (1993).
[11] A. M. Glass, MRS Bull. **13**, 16 (1988).
[12] L. Pauling, *The Nature of the Chemical Bond* (Cornell Univ. Press, Ithaca, NY, 1948), 2nd ed.
[13] E. M. Levin, C. R. Robbins, and H. F. McMurdie, *Phase Diagrams for Ceramists* (The American Ceramic Society, Columbus, OH, 1964).
[14] M. Cotter, S. Cambell, and R. G. Egdell, Surf. Sci. **197**, 208 (1988).
[15] E. A. Colbourn, W. C. Mackrodt, and P. W. Tasker, Physica (Amsterdam) **131B**, 41 (1985).
[16] P. W. Tasker, E. A. Colbourn, and W. C. Mackrodt, J. Am. Ceram. Soc. **68**, 74 (1985).
[17] R. A. McKee, F. J. Walker, and J. Harding (to be published).
[18] J. Harding, R. A. McKee, and F. J. Walker (to be published).
[19] T. Terashima, Y. Bando, K. Iijima, K. Yamamoto, K. Hirata, K. Hayashi, K. Kamigaki, and H. Terauchi, Phys. Rev. Lett. **65**, 2684 (1990).
[20] F. J. Walker, R. A. McKee, Huan-wun Yen, and D. E. Zelmon (to be published).

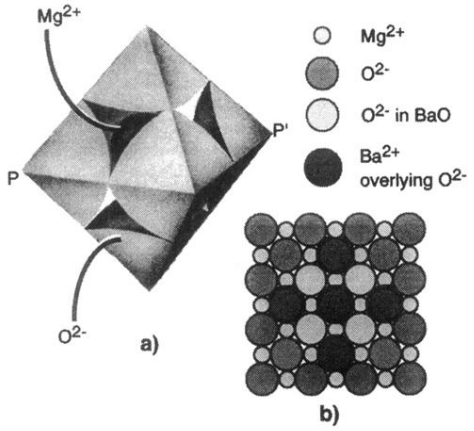

FIG. 1. Size effects, stacking sequence. (a) oxygen oxtahedra showing Mg^{2+} coordination; *P-P'* is [100]; (b) (001)MgO with 45°-rotated BaO layer at anion-anion overlap position.

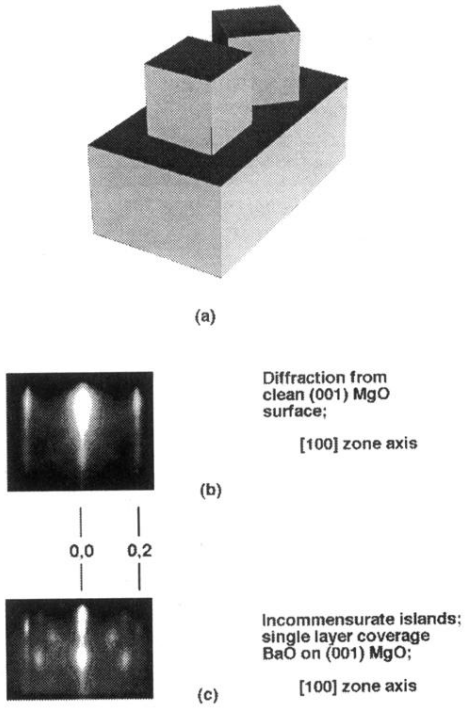

FIG. 2. Incommensurate nucleation and growth of BaO on (001)MgO. (a) Cube model of two orientations; (b) RHEED from the [100] zone axis of clean MgO; (c) RHEED from $\frac{1}{2}$ monolayer BaO-covered MgO.

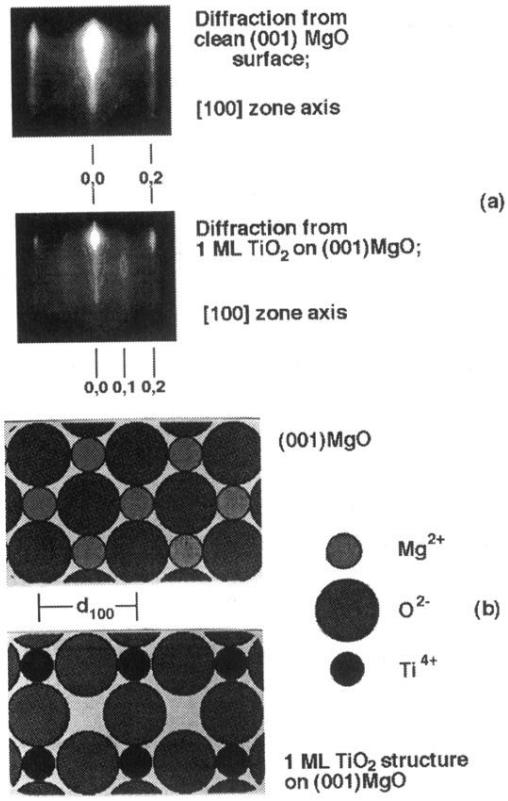

FIG. 3. TiO_2 truncation of (001) MgO. (a) RHEED at the [100] zone axis for clean and TiO_2-truncated MgO; (b) ball models of (001) surfaces.

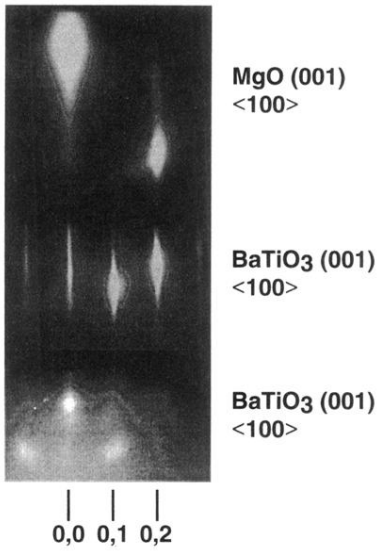

FIG. 4. RHEED data for MgO and $BaTiO_3$. Upper panel: clean MgO (100 nm homoepitaxial growth on polished surface); middle panel: 100 nm $BaTiO_3$ grown on TiO_2-truncated MgO; lower panel: 100 nm $BaTiO_3$ grown on BaO-truncated MgO.